

Supplementary Information

Continuous Fabrication of Plasmonic Photonic Microcapsules with Controllable Metal covered Nanoparticle Arrays using Droplet Microfluidics for Localized Surface Plasmon Resonance

Juan Wang^{abc}, Mingliang Jin^{ab}, Yingxin Gong^{ab}, Hao Li^{ab}, Sujuan Wu^{ab}, Zhang Zhang^{ab},
Guofu Zhou^{ab}, Lingling Shui^{abc*}, Jan C. T. Eijke^{bc} and Albert van den Berg^{bc}

^aInstitute of Electronic Paper Displays, South China Academy of Advanced Optoelectronics,
South China Normal University, Guangzhou 510006, China

^bJoint International Research Laboratory of Optical Information of the Chinese Ministry of
Education, South China Normal University, Guangzhou 510006, China

^cBIOS/Lab-on-a-Chip group, MESA+ Institute for Nanotechnology, University of Twente,
Drienerlolaan 5, 7522 NB Enschede, the Netherlands

*Corresponding author: SHUILL@m.scnu.edu.cn

Optical microscopy measurements

Optical images were taken using an inverted optical microscope (Olympus IX2, Tokyo, Japan) equipped with a high-speed camera (Phantom, MIRO M100, Vision Research Inc., Wayne County, NC, USA) in bright-field mode. Digital camera adapter (DV-500) matched on the metallurgical microscope (L3230, Guangzhou Liss Optical Instrument Co. LTD., China) was used to observe the microcapsules. The average diameter of the emulsion droplets and microparticles was analyzed using Image J software.

Scanning electron microscopy

Fabricated microcapsules suspended in ethanol were dripped onto a silicon substrate and dried by a stream of nitrogen gas. A thin layer (5-10 nm) of Au (Quorum Q150TES, Quorum Technologies Ltd., Ashford, England) was deposited on the microcapsule before SEM measurements if the microcapsule was covered by silica nanoparticles without metal film. The morphology of the nanoparticle on microcapsule was observed by FE-SEM (ZEISS ultra 55, Carl Zeiss, Germany) with an accelerating voltage of 5 kV. The secondary electron mode was used to collect morphology signals.

Reflectance measurements

A fiber optic spectrometer (USB2000, Ocean Optics Inc., Shanghai, China) equipped with a biological microscope (UB200i, COIC Industrial Co., Ltd, Chongqing, China) was used to measure the reflection spectra of photonic crystal microcapsules with nanopatterns.

Calculation of SERS enhancement factor

To estimate the Enhancement Factor (EF) of the particle-laden plasmonic microcapsules (PLPM), pure MBT bulk powder was measured to get the normal Raman spectrum. EF of the produced plasmonic photonic microcapsules (Ag- and Au- covered photonic capsules) was calculated for the SERS peaks at 1078 and 1592 cm^{-1} , respectively, according to the equation $EF = (I_{\text{SERS}}/I_{\text{Bulk}}) \times (N_{\text{Bulk}}/N_{\text{SERS}})$. Where I_{SERS} and I_{Bulk} are the intensities of the same band of the Raman signal from the analytical molecules on the SERS substrate and on pure bulk substrate, respectively, and N_{SERS} and N_{Bulk} are the number of the analytical molecules probed in the Raman spectrum on the SERS substrate and on pure bulk substrate, respectively.

N_{Bulk} was determined based on the Raman spectrum of the solid-state 4-MBT and the focal volume of the Raman system. It was excited on the pure 4-MBT bulk substrate, and N_{Bulk} was determined by assuming that the laser excitation volume has a cylinder shape with the circular diameter being equal to the focused laser spot diameter and the height being equal to the effective probe depth (H_{obj}). H_{obj} was obtained by adjusting the substrate stage out of the laser focus plane in 1 μm increments and capturing the silicon characteristic peak value at 520 cm^{-1} .¹ N_{Bulk} is not counted when the signal intensity is less than half of the maximum value at the characteristic position, yielding the H_{obj} value of 26 μm . The amount of N_{Bulk} that contributes to the pure bulk Raman signal inside the interaction volume is calculated to be 2.46×10^{11} with the molar volume of 4-MBT 118.3 $\text{cm}^3 \text{mol}^{-1}$.

In this work, to avoid the effect from non-SERS area, I_{SERS} is calculated by subtracting the signal of non-SERS area from the measured Raman intensity at the same position, as demonstrated in Fig. S3a (see

details in Table S1). When determining N_{SERS} , the number of the contributory molecules in the "hot-spot" region, the equation $N_{\text{SERS}} = A_s \times D_{4\text{-MBT}}$ is applied, where A_s is the contributory "hot-spot" surface area and $D_{4\text{-MBT}}$ is the surface density of the 4-MBT molecules chemisorbed on the metallic nanostructured surface. 4-MBT molecules are assumed to be absorbed as a monolayer with a surface density ($D_{4\text{-MBT}}$) of 4 molecules nm^{-2} onto the surface area (A_s).^{2, 3} The model shown in Fig. S3b is employed to calculate A_s .⁴ In this calculation, r is the mean radius of silica nanoparticles, and h is the nanogap distance which is assumed to be 5 nm for the nanoparticle, assuming a 378 nm nanoparticle and a 145 nm Ag film thickness. The diameter of the light spot in our Raman system is 1.54 μm , which includes approximately 34 "hot-spot" scattering sites contributed to the SERS signal enhancement based on the SEM images in Fig. 4 in the main manuscript. N_{SERS} was obtained by multiplying the calculated total surface area of the 34 "hot-spots" region ($A_s = 4.03 \times 10^{-13} \text{ m}^2$) by the surface density of the 4-MBT molecules chemisorbed on the nanogap surface ($D_{4\text{-MBT}} = 4 \times 10^{18} \text{ molecules m}^{-2}$), yielding $N_{\text{SERS}} = 1.61 \times 10^6$. The EF of the "hot-spots" was calculated to be 1.3×10^7 and 7.5×10^7 at the Raman shift of 1078 and 1592 cm^{-1} , respectively with $d = 378 \text{ nm}$ and $t_{\text{Ag}} = 145 \text{ nm}$. The maximum enhancement factors on Au-covered microcapsules were 1.1×10^7 and 4.5×10^7 at the Raman shift of 1078 and 1592 cm^{-1} , respectively, with $d = 378 \text{ nm}$ and $t_{\text{Au}} = 198 \text{ nm}$. Corresponding simulation work is described in the following.

Simulation of localized electromagnetic field at the Au- and Ag-covered nanogaps

From previous studies, numerous results show that the noble metal nanoparticle dimer structures could provide strong localized electromagnetic field at the nanogaps of dimers. In order to study the electromagnetic surface mode of the nanoparticle array, called localized surface plasmon polaritons (LSPP), the finite difference time domain (FDTD) simulation was applied. The profile data of Au- and Ag-covered nanoparticles with $d = 378 \text{ nm}$ was applied in the FDTD simulator. Fig. S4 demonstrates the specific electromagnetic field distribution of the Au- and Ag-covered nanogaps, which is consistent with the SERS intensity distribution in previous studies and the measured data.

The electromagnetic field enhancement is extremely large at the specific area (hot spots) between two metal-decorated particles, which is defined as:

$$g(x, z) = \left| \vec{E}_{\text{tot}}(x, z) \right| / \left| \vec{E}_0(x, z) \right|, \quad (1)$$

where $\left| \vec{E}_0(x, z) \right|$ is the electric field of the incident optical excitation with frequency ω_0 . The field enhancement is an important parameter used to assess the electromagnetic SERS enhancement factor EF . The electromagnetic SERS enhancement is a consequence of the enhancement of both the incident electric field and the scattered electric field. Assuming that the enhancement is independent of the absolute photon fluxes and polarizations, the electromagnetic enhancement factor for a Stokes scattering process can be expressed as:⁵

$$EF(\vec{r}, \omega) = \left[\frac{E_{\text{tot}}(\vec{r}, \omega_0)}{E_0(\vec{r}, \omega_0)} \right]^2 \cdot \left[\frac{E_{\text{tot}}(\vec{r}, \omega_0 - \omega_1)}{E_0(\vec{r}, \omega_0 - \omega_1)} \right]^2, \quad (2)$$

where ω_0 is the incident radiation frequency and the scattered radiation has vibrational frequency ω_1 . The electromagnetic field resulted in a Raman scattering enhancement which can be estimated by $EF \approx g^4$. Therefore, the maximum Raman enhancement factor for the Au- and Ag-covered nanoslits are 2.4×10^7 and 1.2×10^8 , respectively, which are in good agreement with the experimental results (1.1×10^7 and 4.5×10^7 at the Raman shift of 1078 and 1592 cm^{-1} for Au-covered nanoarray; 1.3×10^7 and 7.5×10^7 at the Raman shift of 1078 and 1592 cm^{-1} for Ag-covered nanoarray) considering the non-optimum alignment and particle shapes.

Raman measurement of 2-mercaptoethanesulfonate

To demonstrate the efficiency of the particle-laden plasmonic microcapsules, smaller Raman cross-section molecule of 2-mercaptoethanesulfonate (MES) anions have also been tested by chemisorbed to the PLPMs. Sodium 2-mercaptoethanesulfonate like other thiols has high affinity to the silver surface; it strongly binds to Ag nanopatterns through S-H groups and forms a metal-sulfur bond.⁶ The PLPMs were put in 10 mM MESNa aqueous solution for 10 min, and rinsed for 1 min after taken out. After drying using N_2 , the sample was put on the stage for Raman measurement. The 633 nm laser with power of 1% was used for all Raman measurements. Each Raman spectrum was collected for one accumulation in 10 s. The experimental results are shown in Fig. S6. The band of 303 cm^{-1} corresponds to the Ag-S stretching vibrations, according to the previously reported works. The bands at 647, 715 and 808 cm^{-1} arises from C-S stretching vibration. The most intense band at 808 cm^{-1} involves sulfur from the sulfonate group $\nu(\text{C}_1\text{-S})$ (see the carbon numbering in the inset of Fig. S6), whereas the other two bands at 647 and 715 cm^{-1} involve sulfur of the thiol group and can be ascribed to the trans (T) and gauche (G) conformation of S (thiol)-C-C chain (marked as $\nu(\text{C}_2\text{-S})_{\text{T}}$ and $\nu(\text{C}_2\text{-S})_{\text{G}}$, respectively).⁷ The SERS band at 1045 and 1079 cm^{-1} can be assigned to the symmetric stretch of the sulfonate group ($\nu_s(\text{SO}_3^-)$). These bands exhibit the characteristic splitting. The position of the higher wavenumber band is very close to SO_3^- band in the Raman spectrum of crystalline MESNa and varies with the counterion.⁸ Therefore, the 1079 cm^{-1} component has been ascribed to the sulfonate groups interacting with sodium cations directly, while the 1045 cm^{-1} is assigned to solvated SO_3^- groups. The bulk MESNa powder was also measured (the inset of Fig. S6). It is obvious that significant SERS effect was obtained on PLPMs compared to the bulk materials.

References

1. M. Khan, T. Hogan, B. Shanker, *J. Nano Syst. Technol*, 2009, **1**, e11.
2. K. Seo and E. Borguet, *J. Phys. Chem. C*, 2007, **111**, 6335-6342.
3. A. Ulman, *Chem. Rev.*, 1996, **96**, 1533-1554
4. W. Li, P. H. Camargo, X. Lu, Y. Xia, *Nano Lett.*, 2008, **9**, 485-490.
5. A. Otto, M. Cardona, *Top. Appl. Phys.*, 1984, **54**, 289.
6. A. Kudelski, *Langmuir*, 2002, 18 (12): 4741-4747.
7. Z. Zheng, Y. Chen, N. Bi, et al., *Spectrochimica Acta Part A Molecular & Biomolecular Spectroscopy*, 2011, 81(1): 578-582.
8. A. Kudelski, M Pecul, J Bukowska, *Journal of Raman Spectroscopy*, , 2002, 33(33):796-800.

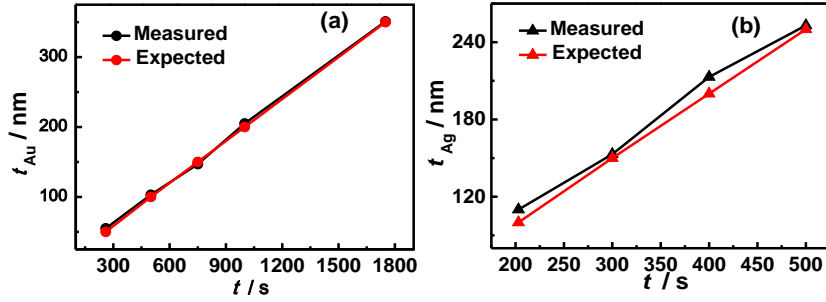


Fig. S1 Curves of expected and measured metal film thickness versus deposition time. (a) Au film thickness (t_{Au}) versus deposition time (t); (b) Ag film thickness (t_{Ag}) versus deposition time (t).

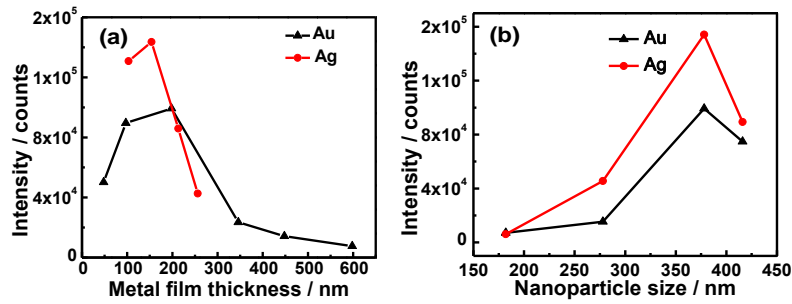


Fig. S2 (a) Raman intensity plotted as a function of Au and Ag film thickness (t_{Au} and t_{Ag}) at $d = 378$ nm. (b) Raman intensity plotted as a function of nanoparticle size (d) at ($t_{Au} = 198$ nm and $t_{Ag} = 145$ nm).

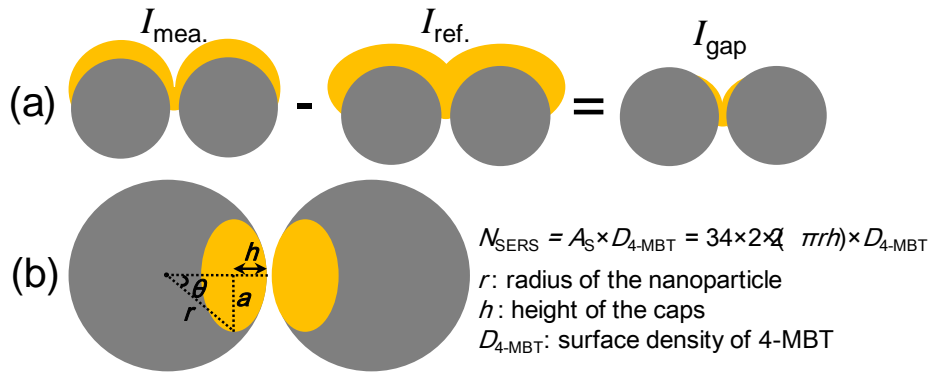


Fig. S3 Schematic drawing of the real nanogap (hot-spot) contributed Raman intensity obtained by subtracting the reference (non-SERS area) surface from the measured intensity (a), and the method to estimate the number of probe molecules trapped in the "hot-spots" (N_{SERS}) among the neighboring nanoparticles (b). The hot-spot region is assumed to comprise a cap on the surface of each nanoparticle in the inter-particle region (orange).

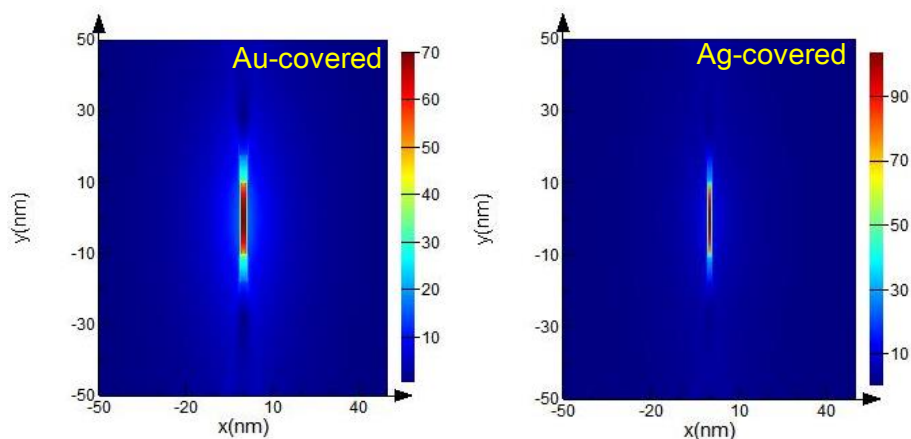


Fig. S4 Simulated localized electromagnetic field in the nanogaps of Au- and Ag-covered SERS nanoarrays using the finite difference time domain (FDTD). The simulated EF_{\max} of Au- and Ag-covered substrates are 2.4×10^7 and 1.2×10^8 , respectively.

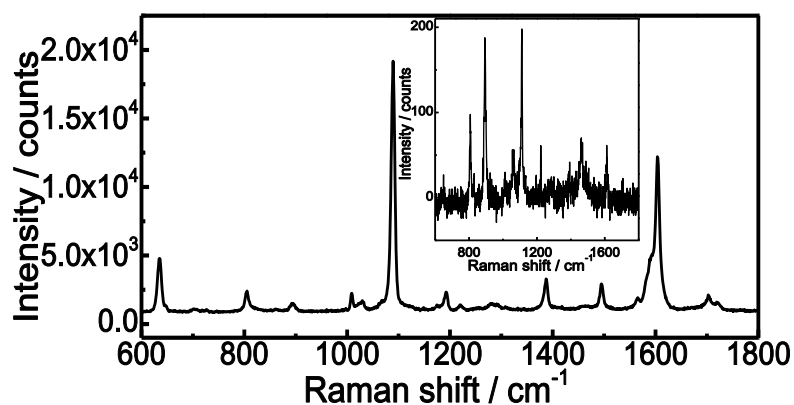


Fig. S5 Measured SERS spectrum of 4-MBT with PLPMs in solution (0.1 mM), with inset the Raman spectrum of 1M 4-MBT aqueous solution without SERS substrate.

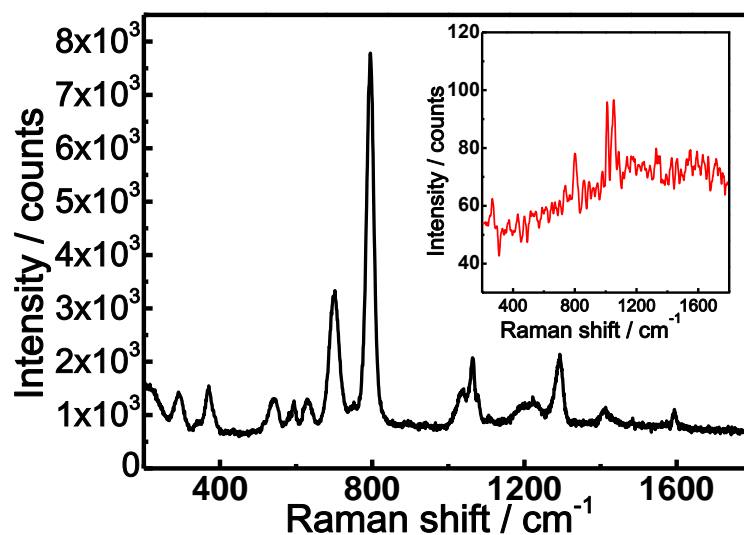


Fig. S6 Measured SERS spectrum of MESNa with PLPMs in solution (0.1 mM), with inset the Raman spectrum of 1M MESNa aqueous solution without SERS substrate.

Table S1 *EF* values of Au- and Ag-covered PLPMs

<i>Raman shift</i> <i>Intensity</i>	<i>Raman shift</i>		<i>Raman shift</i> <i>Intensity</i>	<i>Raman shift</i>	
	1078 cm ⁻¹	1592 cm ⁻¹		1078 cm ⁻¹	1592 cm ⁻¹
$I_{\text{Au-max}}$	99302	48460	$I_{\text{Ag-max}}$	154183	102959
$I_{\text{Au-ref}}$	7604	3944	$I_{\text{Ag-ref}}$	42627	28670
$I_{\text{Au-gap}}$	91698	44516	$I_{\text{Ag-gap}}$	111556	74289
EF_{Au}	1.1×10^7	4.5×10^7	EF_{Ag}	1.3×10^7	7.5×10^7

Note: I_{max} is the maximum intensity Raman peaks at 1078 and 1592 cm⁻¹; I_{ref} is the reference intensity from flat Au or Ag film; I_{gap} is the Raman intensity from the nanogaps by abstracting I_{ref} from I_{max} .

Table S2 Raman intensity ratio of Au-covered PLPMs to flat Au film

t_{Au} (nm)	$I_{\text{PLPM}} 1076 \text{ cm}^{-1}$	$I_{\text{ratio}}(1076)=I_{\text{PLPM}}/I_{\text{film}}$	$I_{\text{PLPM}} 1592 \text{ cm}^{-1}$	$I_{\text{ratio}}(1592)=I_{\text{PLPM}}/I_{\text{film}}$
Au flat film	3.2	/	1.4	/
48	50195.7	1.6×10^4	30888.4	2.2×10^4
97	89537.5	2.8×10^4	44635.5	3.2×10^4
198	99301.6	3.1×10^4	48460.2	3.5×10^4
346	23543.9	7.4×10^3	9992.75	7.1×10^3
448	14276.4	4.5×10^3	7270.02	5.2×10^3
598	7604.07	2.4×10^3	3944.4	2.8×10^3

Table S3 Raman intensity ratio of Ag-covered PLPMs to flat Ag film

t_{Au} (nm)	$I_{\text{PLPM}} 1076 \text{ cm}^{-1}$	$I_{\text{ratio}}(1076)=I_{\text{PLPM}}/I_{\text{film}}$	$I_{\text{PLPM}} 1592 \text{ cm}^{-1}$	$I_{\text{ratio}}(1592)=I_{\text{PLPM}}/I_{\text{film}}$
Ag flat film	5.2	/	5.6	/
103	130842	2.5×10^4	70203	1.3×10^4
154	143582	2.8×10^4	84908	1.5×10^4
213	85897	1.7×10^4	49419	8.8×10^3
256	42627	8.2×10^3	28670	5.1×10^3